

 Open access • Journal Article • DOI:10.1002/CHEM.201805680

Heterogeneous Metal–Organic-Framework-Based Biohybrid Catalysts for Cascade Reactions in Organic Solvent — [Source link](#)

Yangxin Wang, Yangxin Wang, Ningning Zhang, En Zhang ...+5 more authors

Institutions: Northwestern Polytechnical University, Dresden University of Technology, Tsinghua University, University of Southern Denmark

Published on: 01 Feb 2019 - Chemistry: A European Journal (John Wiley & Sons, Ltd)

Topics: Metal-organic framework, Catalysis, Heterogeneous catalysis and Ethyl hexanoate

Related papers:

- [Metal-Organic Frameworks for CO₂ Chemical Transformations.](#)
- [A Stable Metal-Organic Framework Featuring a Local Buffer Environment for Carbon Dioxide Fixation.](#)
- [Co-immobilization of an Enzyme and a Metal into the Compartments of Mesoporous Silica for Cooperative Tandem Catalysis: An Artificial Metalloenzyme](#)
- [Design of a Highly-Stable Pillar-Layer Zinc\(II\) Porous Framework for Rapid, Reversible, and Multi-Responsive Luminescent Sensor in Water](#)
- [A porous metal–organic framework formed by a V-shaped ligand and Zn\(II\) ion with highly selective sensing for nitroaromatic explosives](#)

Share this paper:    

View more about this paper here: <https://typeset.io/papers/heterogeneous-metal-organic-framework-based-biohybrid-2xasvdpgti>



University of Southern Denmark

Heterogeneous Metal–Organic-Framework-Based Biohybrid Catalysts for Cascade Reactions in Organic Solvent

Wang, Yangxin; Zhang, Ningning; Zhang, En; Han, Yunhu; Qi, Zhenhui; Ansorge-Schumacher, Marion B.; Ge, Yan; Wu, Changzhu

Published in:
Chemistry: A European Journal

DOI:
10.1002/chem.201805680

Publication date:
2019

Document version:
Accepted manuscript

Citation for polished version (APA):
Wang, Y., Zhang, N., Zhang, E., Han, Y., Qi, Z., Ansorge-Schumacher, M. B., Ge, Y., & Wu, C. (2019). Heterogeneous Metal–Organic-Framework-Based Biohybrid Catalysts for Cascade Reactions in Organic Solvent. *Chemistry: A European Journal*, 25(7), 1716-1721. <https://doi.org/10.1002/chem.201805680>

Go to publication entry in University of Southern Denmark's Research Portal

Terms of use

This work is brought to you by the University of Southern Denmark.
Unless otherwise specified it has been shared according to the terms for self-archiving.
If no other license is stated, these terms apply:

- You may download this work for personal use only.
- You may not further distribute the material or use it for any profit-making activity or commercial gain
- You may freely distribute the URL identifying this open access version

If you believe that this document breaches copyright please contact us providing details and we will investigate your claim.
Please direct all enquiries to puresupport@bib.sdu.dk



Author Manuscript

Title: Heterogeneous metal-organic frameworks-based biohybrid catalysts for cascade reaction in organic solvent

Authors: Yangxin Wang, Dr.; Ningning Zhang; En Zhang; Yunhu Han; Zhenhui Qi, Dr.; Marion Ansorge-Schumacher, Dr.; Yan Ge; Changzhu Wu, Ph.D.

This is the author manuscript accepted for publication and has undergone full peer review but has not been through the copyediting, typesetting, pagination and proofreading process, which may lead to differences between this version and the Version of Record.

To be cited as: 10.1002/chem.201805680

Link to VoR: <https://doi.org/10.1002/chem.201805680>

Heterogeneous metal-organic frameworks-based biohybrid catalysts for cascade reaction in organic solvent

Yangxin Wang,^[a, b] Ningning Zhang,^[b] En Zhang,^[c] Yunhu Han,^[d] Zhenhui Qi,^{*[a]} Marion B. Ansorge-Schumacher,^{*[b]} Yan Ge,^{*[a]} and Changzhu Wu^{*[e]}

Abstract: In cooperative catalysis, the combination of chemo- and biocatalysts to perform one-pot synthetic route is a powerful tool for the improvement of chemical synthesis. Herein, UiO-66-NH₂ was employed to stepwise immobilize Pd nanoparticles (NPs) and *Candida antarctica* lipase B (CalB) for the fabrication of biohybrid catalysts for cascade reaction. Distinct from traditional materials, UiO-66-NH₂ has a robust but tunable structure which can be utilized with a ligand exchange approach to adjust its hydrophobicity, resulting in excellent catalyst dispersity in diverse reaction media. These attractive properties eventually contribute the MOF-based biohybrid catalysts with high activity and selectivity in the synthesis of benzyl hexanoate from benzaldehyde and ethyl hexanoate. With this proof-of-concept, we reasonably expect that future tailor-made MOFs can combine more other catalysts, ranging from chemical to biological catalysts for perspective applications in industry.

Nature has evolved to create biohybrid catalysts, through the integration of biocatalysts into biological scaffolds, to proceed cooperative biotransformation in cellular machinery.^[1] The value of scaffolds is to provide spatial restriction and close confinement around catalysts, which facilitates cascade bioreactions in a cooperative and efficient fashion while minimizing the decomposition of active intermediates.^[2] An example of such cooperativity is carboxysomes, which harbor two distinct enzymes in protein cages for the efficient CO₂ fixation.^[3] This intriguing nature design has initiated great efforts

in bioinspired synthetic chemistry.^[4]

In this context, considerable progress has been made to mimic biohybrid structure for remarkable cascade catalysis. These include DNA-hybrid catalysts,^[5] protein-based compartments,^[6] liposomes,^[7] artificial metalloenzymes,^[8] and polymer-based capsules,^[9] which have been extensively reviewed in the literature.^[10] Most of these catalysts are fabricated by simultaneous or stepwise enzyme(s) loading into self-assembled capsules that are typically water-soluble and mechanically soft. Accordingly, they act as flexible cell-mimics in water, producing system-level essential bioproducts from cascade reactions.^[9d] However, these “soft” biohybrid capsules are often limited by their mechanic vulnerability, encountering difficulties in catalyst recycling and process operation. Moreover, they are typically solvent-incompatible, thus are unable to proceed biotransformation where nonpolar substances are used. These limitations present a great challenge to bring “soft” biohybrid catalysts into industry.

To face the challenge, using mechanically robust scaffolds becomes an alternative choice for biohybrid catalysts. In a pioneering study, the Bäckvall group has promoted “hard” biohybrid catalysts by embedding enzymes and metal nanoparticles (NPs) into mesoporous silica.^[11] This design allows two active species to cooperatively catalyze dynamic kinetic resolution in a solid matrix, which behaves similarly to the cooperativity in these “soft” cell-mimics (e.g., liposomes). The difference, however, is the use of solid carriers that facilitates catalyst reuse while allowing to be performed in various reactions media, including water, organic solvents, and even aqueous-organic two-phase.^[12] To date, a variety of solid particles have been utilized for the fabrication of biohybrid catalysts, ranging from silica^[13] to reduced graphene oxide^[14] and polymeric matrix^[15]. Despite this, unlike soft matters, these solid supports only act as inert and “hard” carriers that have physically fixed structure, thus lack of structure flexibility and tunability which are crucial factors to the regulation of catalytic performances. Therefore, up to now, a fundamental gap between robustness and tunability remains when designing applicable biohybrid catalysts.

To fill this gap, we herein report for the first time metal-organic frameworks (MOFs)-based biohybrid catalysts where metal catalysts (Pd NPs) and biocatalysts (*Candida antarctica* lipase B) are respectively immobilized in distinct compartments for cascade catalysis. As a coordination network, MOFs represent a fascinating platform whose structure, porosity and functionality can be finely tuned by judicious design of metal nodes and organic linkers^[16] or through post-synthetic methods.^[17] MOFs have shown great potential in the field of both chemocatalysis^[18] and biocatalysis.^[16d, 19] Incorporating two catalysts into MOFs, therefore, provides the biohybrid with sufficient robustness for catalyst recycling, and tunable porous structure for substance

[a] Dr. Y. Wang, Associate Prof. Y. Ge, Prof. Z. Qi
Sino-German Joint Research Lab for Space Biomaterials and
Translational Technology, School of Life Sciences
Northwestern Polytechnical University
127 Youyi Xilu, Xi'an, Shaanxi 710072, P. R. China
E-mail: ge@nwpu.edu.cn; qi@nwpu.edu.cn

[b] Dr. Y. Wang, N. Zhang, Prof. M. B. Ansorge-Schumacher
Institute of Microbiology
Technische Universität Dresden
Zellescher Weg 20b, 01217 Dresden, Germany
E-mail: marion.ansorge@tu-dresden.de

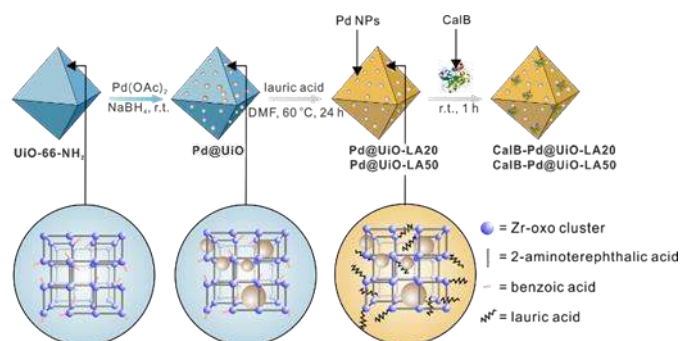
[c] E. Zhang
Department of Chemistry
Technische Universität Dresden
Bergstraße 66, 01062 Dresden, Germany

[d] Y. Han
Department of Chemistry
Tsinghua University
Beijing 100084, China

[e] Prof. C. Wu
Danish Institute for Advanced Study (DIAS) and Department of
Physics, Chemistry and Pharmacy
University of Southern Denmark
5230 Odense, Denmark
E-mail: wu@sdu.dk

Supporting information for this article is available on the WWW
under <http://dx.doi.org/10.1002/chem.2018xxxxx>.

diffusion.^[20] As is known, Pd NPs have been widely used as catalyst in different types of reactions, such as reduction, oxidation, racemization, and coupling reactions.^[21] While CalB is a well-known and easily available lipase which can efficiently catalyze esterification, hydrolysis, and transesterification reactions in a mild manner.^[19m, 22] Therefore, various cascade reactions can be achieved through the cooperative application of Pd NPs and CalB. However, mutual inactivation of chemo- and biocatalysts was regularly found in metal-containing biohybrid catalysts, which inhibits their catalytic performances. In this context, precise synthesis with MOFs as supporting carrier would allow the chemo- and biocatalysts compartmentalized in different locations, avoiding their mutual inactivation. The tiny Pd NPs will be stabilized in the inner pores of MOFs, while CalB will be immobilized on the surface of MOFs because of its larger sizes (6.9 nm × 5.0 nm × 8.7 nm).^[23] Moreover, with a ligand exchange method, the surface hydrophobicity of MOFs catalysts can be tailor-made to adapt to many reaction media of interests. Therefore, we have proved the concept that a robust and tunable MOFs platform can be developed to compartmentalize diverse catalysts for the efficient cascade biotransformation.



Scheme 1. Schematic illustration of the synthesis of CalB-Pd@UiO-LA20 and CalB-Pd@UiO-LA50.

In this work, UiO-66-NH₂ was chosen as “hard” scaffold owing to its high stability and ready post-functionality.^[24] Excess benzoic acid was added during preparing UiO-66-NH₂ following reported protocol,^[25] because it could not only lead to MOFs with small sizes,^[26] but also offer the opportunities for post-modification through ligand exchange.^[27] Initially, the as-synthesized UiO-66-NH₂ was employed for ligand exchange. The reaction was performed in DMF solution of lauric acid (50 mM), and the product was denoted as UiO-LA50. As shown in Figure S1, water contact angle of UiO-LA50 is 112.2 ± 1.6 °, which is much larger than that of the pristine UiO-66-NH₂, indicating the success of ligand exchange. But considering that the ligand exchange has an influence on the surface property of MOF materials, it may further influence the amount of subsequently immobilized Pd NPs, herein, for the convenience of comparing the catalytic performances of the biohybrid catalysts, Pd NPs were immobilized on MOFs before the ligand exchange. The procedure of immobilizing Pd NPs and CalB in/on hydrophobized MOFs is depicted in Scheme 1. To tune the hydrophobicity of Pd@UiO, lauric acid was applied for ligand

exchange in DMF solution, obtaining products Pd@UiO-LA20 and Pd@UiO-LA50, during which 20 and 50 mM lauric acid were used, respectively. After ligand change, water contact angle of Pd@UiO increased from 16.3 ± 2.2 ° to 26.9 ± 2.3 ° (Pd@UiO-LA20) and 133.5 ± 1.4 ° (Pd@UiO-LA50) (Figure. 1a). This hydrophobicity upsurge suggests that the surface composition of Pd@UiO has been finely tuned. The ligand exchange was further confirmed by analyzing components released from Pd@UiO, Pd@UiO-LA20, and Pd@UiO-LA50 with gas chromatography coupling with mass spectrometry (GC/MS) (Figure. S2). The molecular ion peak at *m/z* = 200 clearly supports the existence of lauric acid in Pd@UiO-LA20 and Pd@UiO-LA50, but not in Pd@UiO. In order to quantify the respective content of ligands in the MOF-based materials after ligand exchange, the MOF-based materials were digested in deuterium DMSO containing hydrofluoric acid, and then characterized with ¹H NMR. As shown in Figure S3, peaks from benzoic acid and 2-aminoterephthalic acid are observed in the spectra of digested pristine UiO-66-NH₂ and Pd@UiO, and peaks from lauric acid appears in the spectra of digested Pd@UiO-LA20 and Pd@UiO-LA50, which again confirms the successful ligand exchange. There are also some unidentified peaks observed in the aromatic region in all the spectra of digested MOF-based materials. These peaks are presumably derived from the 2-aminoterephthalic acid.^[28] Nevertheless, the molar ratio of lauric acid to benzoic acid in Pd@UiO-LA20 and Pd@UiO-LA50 can be estimated from their peak areas, which is about 0.69 and 0.92, respectively.

To prepare biohybrid catalysts for cascade reactions, CalB was physically adsorbed onto Pd@UiO, Pd@UiO-LA20, and Pd@UiO-LA50, obtaining biohybrid catalysts, CalB-Pd@UiO, CalB-Pd@UiO-LA20, and Cal-Pd@UiO-LA50, respectively. This preparation allows to spatially separate Pd NPs in MOFs from enzymes on the surface, thus benefiting by circumventing possible mutual inactivation that often occurs between chemo- and biocatalysts.^[29] Bradford assay disclosed that CalB loaded onto CalB-Pd@UiO, CalB-Pd@UiO-LA20, and CalB-Pd@UiO-LA50 was 7.2, 16.8, and 12.1 mg g⁻¹, respectively (Figure. S4). No measurable amount of CalB from all these MOF-based catalysts was detected in leaching test, suggesting that the protein is strongly attached to the carriers (details in item 1.8, supporting information). CalB-Pd@UiO-LA50 shows the remarkable capability to disperse in different organic solvents of a wide range of polarity (Figure. S5), implying that this MOF-based biohybrid catalyst could be applied in various reaction media of interests, which is an important achievement with respect to reaction media engineering. We examined the changes of zeta potential (ζ -potential) of MOF-based catalysts in the presence of different concentrations of CalB (Figure 1b). When there is no CalB, ζ -potential of Pd@UiO, Pd@UiO-LA20, and Pd@UiO-LA50 is 19.5±0.9, 13.8±0.6, and 12.9±0.3 mV, respectively. With the increasing concentration of CalB in solution, ζ -potential gradually decreases because the positive charge is neutralized by the negative charge of CalB. When the concentration of CalB reaches above 15.8 $\mu\text{g mL}^{-1}$, ζ -potential approaches to an equilibrium plateau. These results suggests that coulombic forces should play an important role in the immobilization of CalB, which corroborates well with the findings by Hupp and colleagues.^[30] Meanwhile, the hydrophobicity of the

MOF materials also has an impact on the immobilization of CalB, as hydrophobic interactions between carriers and enzymes are regarded as a convenient and effective way for enzyme immobilization.^[31] Elemental analysis and inductively coupled plasma atomic emission spectroscopy (ICP-AES) characterization were performed to analyze the chemical components of the MOF-based materials, and the results are summarized in Table S2. Pd content in CalB-Pd@UiO, CalB-Pd@UiO-LA20, and Cal-Pd@UiO-LA50 was determined to be 28.7, 26.6, and 23.4 mg g⁻¹, respectively. The slight variation of Pd content may be caused by the trapped guest molecules, ligand exchange process and enzyme immobilization.

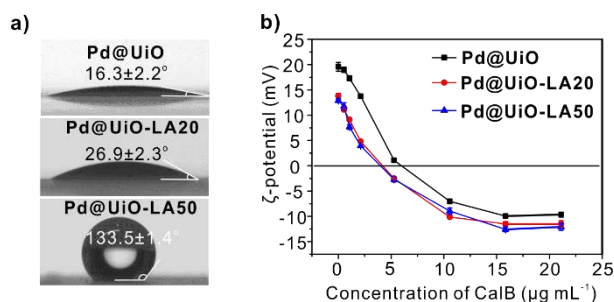


Figure 1. (a) Water contact angle images of Pd@UiO, Pd@UiO-LA20, and Pd@UiO-LA50; (b) Zeta potential of Pd@UiO, Pd@UiO-LA20, and Pd@UiO-LA50 in the presence of CalB at 25 °C.

Thermogravimetric analysis (TGA), powder X-ray diffraction (PXRD) and Fourier transform infrared spectroscopy (FTIR) analysis were carried out, and the results show that the thermal stability, crystallinity and characteristic vibration peaks of pristine UiO-66-NH₂ are well conserved after loading Pd NPs, ligand change and immobilizing CalB (Figure S6, S7, and S8). Based on N₂ adsorption/desorption measurements, the total amount of adsorbed N₂, pore volume and Brunauer-Emmett-Teller (BET) surface areas all decrease slightly after immobilizing CalB (Figure S9 and Table S1). The decrease suggests the presence of proteins on MOFs surface, probably blocking a small portion of their porous cavities. According to the pore size distribution curves, the pore diameter of all the MOF-based materials is smaller than 5 nm, which proves that CalB (6.9 nm × 5.0 nm × 8.7 nm) should be immobilized on the surface of the MOFs.

Scanning electron microscope (SEM) images display that all MOF-based samples are composed of tiny particles with an average diameter of about 100 nm (Figure 2a and S10). These nanoscale particle sizes are beneficial for reducing mass-transfer limitations compared to micron-sized particles. Pd NPs in CalB-Pd@UiO, CalB-Pd@UiO-LA20, and CalB-Pd@UiO-LA50 are clearly observed in transmission electron microscope (TEM) images (Figure 2b and S11). The average diameter of Pd NPs is 3.41 ± 0.49 nm, which is similar to the previously reported Pd NPs supported in MOF materials.^[32] High-angle annular dark-field scanning transmission electron microscopy (HAADF-STEM) and elemental mapping images demonstrate the homogeneous distribution of Pd elements throughout the supports without obvious aggregation (Figure S12).

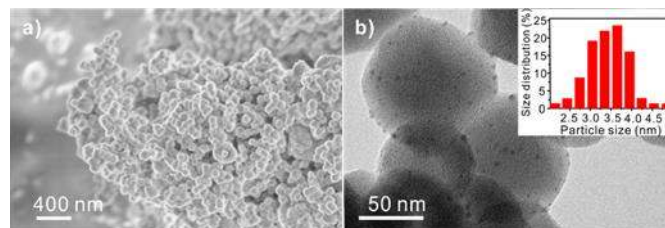


Figure 2. (a) SEM image of CalB-Pd@UiO-LA50; (b) TEM image of CalB-Pd@UiO-LA50 (inset: particle size distribution of Pd NPs).

To ascertain the details of chemical state of Pd NPs, X-ray photoelectron spectroscopy (XPS) measurements were carried out. As shown in Figure S13, the Pd 3d region is divided into two spin-orbital pairs, indicating the presence of two types of surface-bound palladium species. The binding energy peaks at 341.5 (Pd 3d_{5/2}) and 336.0 (Pd 3d_{3/2}) are ascribed from Pd(0) species, while the peaks at 343.4 (Pd 3d_{5/2}) and 337.8 (Pd 3d_{3/2}) are assigned to Pd(II) species. The ratio of Pd(0)/Pd(II) in Pd@UiO is 1.18, estimated from corresponding peak areas. However, it decreases to 0.47 and 0.30 in Pd@UiO-LA20 and Pd@UiO-LA50, respectively. The Pd(II) species may be derived from the reoxidation of Pd(0) during the air contact.^[33] The similar tendency was also observed that the ratio of Pd(0)/Pd(II) in CalB-Pd@UiO-20 and CalB-Pd@UiO-LA50 is 0.34 and 0.46, respectively, while the value is 1.05 in CalB-Pd@UiO.

To visually prove the proteins were adsorbed on the surface of MOFs, CalB was labeled with fluorescein isothiocyanate (FITC), and subjected to the same procedure for preparing CalB-Pd@UiO-LA50. Optical and fluorescence microscopic images reveal that fluorescent CalB readily resided on MOFs after the immobilization (Figure 3). Pd@UiO-LA50 was also incubated in a solution of FITC, which only shows almost invisible fluorescence after washed, excluding the possible influence of FITC on the adsorption behavior of labeled CalB (Figure S14). Interestingly, in addition to CalB, other functional proteins like green fluorescent protein (GFP) and FITC-labelled glucose oxidase (GOD) could be also adsorbed onto Pd@UiO-LA50 using the same method. We notice that the isoelectric points (pI) of GFP (pI = 5.8), GOD (pI = 4.3) and CalB (pI = 5.0) are all negatively charged in neutral pH condition, indicating that it is a relatively general phenomenon for Pd@UiO-LA50 to adsorb negatively charged proteins. Therefore, the successful immobilization of three distinct proteins indicates that MOFs can be developed into a versatile tool for constructing biohybrid catalysts from different biocatalyst sources.

Benzyl alcohol is an important precursor for synthesis of esters in cosmetics and flavouring industries, and is also generally used as solvent for inks and paints.^[34] Reducing benzaldehyde with molecular hydrogen involving Pd catalyst has turned out to be a desirable way to produce benzyl alcohol due to its high efficiency, minimum side reactions and environmental friendliness.^[35] Bearing this in mind, the catalytic performance of Pd@UiO, Pd@UiO-LA20, and Pd@UiO-LA50 without CalB was initially evaluated through the hydrogenation of benzaldehyde in toluene at room temperature. As shown in Figure S15, when the reaction was performed with 0.05 mmol benzaldehyde and 20

mg solid catalyst in toluene, the turnover frequency (TOF) was 28.7, 16.3, and 14.8 h⁻¹ for Pd@UiO, Pd@UiO-LA20, and Pd@UiO-LA50, respectively. It was found that the TOF decreased with the increment of hydrophobicity of catalysts. This is probably due to that the reduction reaction is prohibited by the lipophilic environment in hydrophobized MOF-based catalysts.^[27b]

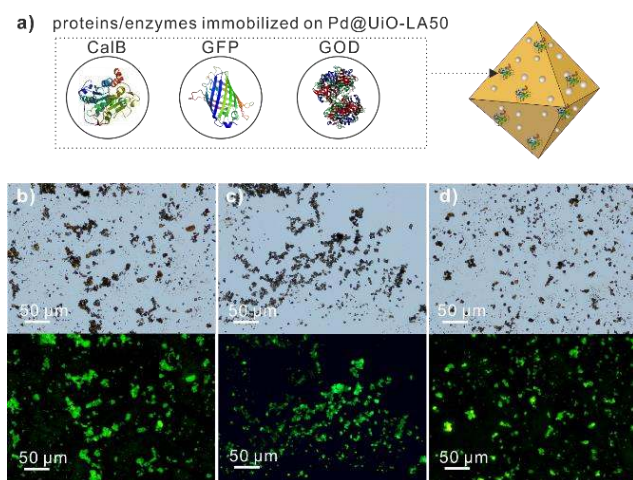


Figure 3. (a) Schematic shows that diverse proteins/enzymes could be immobilized on the Pd@UiO-LA50. Optical (top) and fluorescence (bottom) microscopic images of Pd@UiO-LA50 after adsorbing (b) FITC labeled CalB, (c) GFP, and (d) FITC labeled GOD.

To demonstrate the merit of our MOF-based biohybrid catalysts, a one-pot, two-step cascade reaction transferring benzaldehyde into benzyl hexanoate was then chosen as a model reaction (Figure 4a). Benzaldehyde was first reduced by molecular hydrogen catalysed by Pd NPs into benzyl alcohol, which then reacted with ethyl hexanoate catalysed by CalB to produce benzyl hexanoate. This strategy offers an expedient route to prepare esters for cosmetics or flavouring in one pot directly from benzaldehyde in a mild manner. The reaction was performed in toluene because lipophilic solution is favourable for transesterification reaction. The curves of time-dependent yield of benzyl hexanoate catalysed by different catalysts are given in Figure 4b. When using CalB-Pd@UiO-LA50, an excellent yield of 92% of benzyl hexanoate was achieved in 6 h, and a 100% yield was obtained when reaction time was prolonged to 8 h. While the yield was only about 76% when either CalB-Pd@UiO or CalB-Pd@UiO-LA20 was used at 8 h, respectively. By taking a close look at the reaction, the yield of benzyl hexanoate for CalB-Pd@UiO, CalB-Pd@UiO-LA20, and CalB-Pd@UiO-LA50 at initial 2 h is 17%, 22%, and 52%, respectively. In this regard, CalB-Pd@UiO-LA50 obviously exhibits higher catalytic efficiency than CalB-Pd@UiO and CalB-Pd@UiO-LA20. Considering the almost same catalyst loading, the increased catalytic efficiency in CalB-Pd@UiO-LA50 than others should be due to its improved dispersibility in solvent. Accordingly, this proves the concept that the tunability of MOFs structure can be utilized for efficient catalysis. In control experiments, hydrophobized MOFs without loading CalB (Pd@UiO-LA50) or Pd NPs (CalB@UiO-

LA50, details in item 1.6, supporting information) were also employed as catalysts for the same reaction. However, only benzyl alcohol was observed as a product when Pd@UiO-LA50 was used, and not any product was observed when CalB@UiO-LA50 was applied, illustrating the necessity of cooperation of Pd NPs and CalB for this cascade reaction (Figure S16). Moreover, physically mixed Pd@UiO-LA50 and free CalB was also employed to catalyze the cascade reaction. As shown in Figure S17, the yield of final product benzyl hexanoate is lower than that catalyzed by CalB-Pd@UiO-LA50, possibly due to the aggregation of free CalB in toluene, indicating the superiority of immobilizing enzyme on the MOFs. Another important advantage of the enzyme immobilization is the reusability, since free CalB is difficult to recover from the reaction mixture. As solid heterogeneous catalyst, reusability of CalB-Pd@UiO-LA50 was investigated. After used for three times, the yield of benzyl hexanoate was still maintained about 80% compared with that of the first run (Figure S18). Leaching test after the first run showed that the leaching Pd into reaction solution was only 1.08% out of the original CalB-Pd@UiO-LA50, while no obvious leaching of CalB was observed based on Bradford test. Structural stability of our MOF-based catalyst was further confirmed from the unchanged FTIR spectrum of reused CalB-Pd@UiO-LA50 (Figure S19). TEM image shows that the average diameter of Pd NPs in CalB-Pd@UiO-LA50 after used for 4 times increased slightly to 4.92±1.44 nm, but no obvious aggregation of NPs was observed (Figure S20). Therefore, it is deduced that the enzyme deactivation should be mainly accounted for the degradation of catalytic performance during reuse. To confirm this, CalB-Pd@UiO-LA50 after used for four times in cascade reactions was applied to catalyze the transesterification reaction between benzyl alcohol and ethyl hexanoate. As shown in Figure S21, the activity of reused CalB-Pd@UiO-LA50 is much lower than that of fresh one, indicating the denaturation of CalB during the cascade reactions.

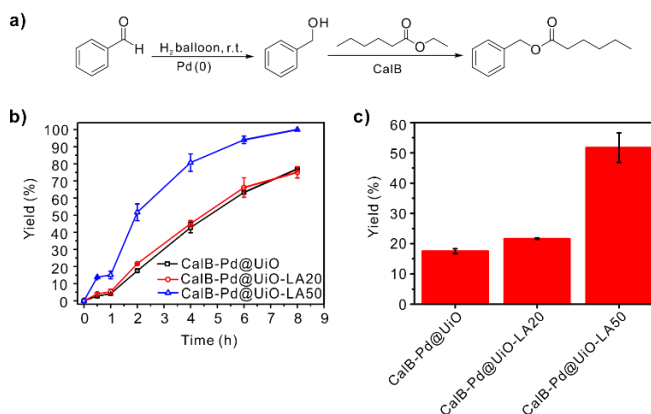


Figure 4. (a) one-pot cascade reaction to produce benzyl hexanoate from benzaldehyde and ethyl hexanoate; (b) Time-dependent yield of benzyl hexanoate catalysed by different biohybrid catalysts; (c) Yield of benzyl hexanoate catalysed by different biohybrid catalysts at 2 h.

In summary, we describe for the first time the use of MOFs as robust and tunable scaffolds for the construction of biohybrid

catalysts, in which Pd NPs and CalB were stepwise immobilized in/on different compartments. The carrier in use, UiO-66-NH₂, is featuring with high tunability and extraordinary robustness, thus allowing the postmodification and multiple reuse in catalysis. In particular, the structure tunability of UiO-66-NH₂ is fully exploited through ligand exchange, creating optimal hydrophobicity of the MOF-based catalyst with wide dispersion in various organic solvents. On a broader perspective, these successful demonstrations open new avenues in the field of biohybrid catalysts where a plateau of other chemo- and biocatalysts and MOFs structures can be further explored. Furthermore, the heterogeneous MOF-based hybrid catalysts were successfully applied for one-pot cascade reaction with high efficiency. This proof-of-principle example suggests the fascinating perspectives of MOF-based catalysts towards more advanced applications in the future.

Acknowledgements

The Thousand Talents Program (1800-16GH030121), China Postdoctoral Science Foundation (2017M623231), Fundamental Research Funds for the Central Universities (3102018zy051), and DFG (WU 814/1-1) are acknowledged.

Keywords: heterogeneous catalysis • metal-organic frameworks (MOFs) • enzyme immobilization • cascade reactions • Pd nanoparticles

- [1] Z. H. Zhou, D. B. McCarthy, C. M. O'Connor, L. J. Reed, J. K. Stoops, *Proc. Natl. Acad. Sci. USA* **2001**, *98*, 14802-14807.
- [2] B. Worsdorfer, K. J. Woycechowsky, D. Hilvert, *Science* **2011**, *331*, 589-592.
- [3] W. Bonacci, P. K. Teng, B. Afonso, H. Niederholtmeyer, P. Grob, P. A. Silver, D. F. Savage, *Proc. Natl. Acad. Sci. USA* **2012**, *109*, 478-483.
- [4] a) M. Filice, J. M. Palomo, *ACS Catal.* **2014**, *4*, 1588-1598; b) J. Muschiol, C. Peters, N. Oberleitner, M. D. Mihovilovic, U. T. Bornscheuer, F. Rudroff, *Chem. Commun.* **2015**, *51*, 5798-5811; c) C. Hold, S. Billerbeck, S. Panke, *Nat. Commun.* **2016**, *7*, 12971; d) K. S. Rabe, J. Muller, M. Skoupi, C. M. Niemeyer, *Angew. Chem. Int. Ed.* **2017**, *56*, 13574-13589; e) X. Liu, D. Appelhans, B. Voit, *J. Am. Chem. Soc.* **2018**, DOI: 10.1021/jacs.8b07980.
- [5] W. Meng, R. A. Muscat, M. L. McKee, P. J. Milnes, A. H. El-Sagheer, J. Bath, B. G. Davis, T. Brown, R. K. O'Reilly, A. J. Turberfield, *Nat. Chem.* **2016**, *8*, 542-548.
- [6] a) T. W. Giessen, P. A. Silver, *ChemBioChem* **2016**, *17*, 1931-1935; b) M. Brasch, R. M. Putri, M. V. de Ruiter, D. Luque, M. S. Koay, J. R. Caston, J. J. Cornelissen, *J. Am. Chem. Soc.* **2017**, *139*, 1512-1519.
- [7] a) R. Matsumoto, M. Kakuta, T. Sugiyama, Y. Goto, H. Sakai, Y. Tokita, T. Hatazawa, S. Tsujimura, O. Shirai, K. Kano, *Phys. Chem. Chem. Phys.* **2010**, *12*, 13904-13906; b) L. Hosta-Rigau, M. J. York-Duran, Y. Zhang, K. N. Goldie, B. Stadler, *ACS Appl. Mater. Interfaces* **2014**, *6*, 12771-12779.
- [8] a) V. Kohler, Y. M. Wilson, M. Durrenberger, D. Ghislieri, E. Churakova, T. Quinto, L. Knorr, D. Haussinger, F. Hollmann, N. J. Turner, T. R. Ward, *Nat. Chem.* **2013**, *5*, 93-99; b) D. F. Sauer, T. Himiyama, K. Tachikawa, K. Fukumoto, A. Onoda, E. Mizohata, T. Inoue, M. Boccola, U. Schwaneberg, T. Hayashi, J. Okuda, *ACS Catal.* **2015**, *5*, 7519-7522; c) Y. Okamoto, V. Kohler, T. R. Ward, *J. Am. Chem. Soc.* **2016**, *138*, 5781-5784.
- [9] a) D. M. Vriezema, P. M. Garcia, N. Sancho Oltra, N. S. Hatzakis, S. M. Kuiper, R. J. Nolte, A. E. Rowan, J. C. van Hest, *Angew. Chem. Int. Ed.* **2007**, *46*, 7378-7382; b) P. Tanner, O. Onaca, V. Balasubramanian, W. Meier, C. G. Palivan, *Chem. Eur. J.* **2011**, *17*, 4552-4560; c) X. Liu, P. Formanek, B. Voit, D. Appelhans, *Angew. Chem. Int. Ed.* **2017**, *56*, 16233-16238; d) H. Tan, S. Guo, N. D. Dinh, R. Luo, L. Jin, C. H. Chen, *Nat. Commun.* **2017**, *8*, 663.
- [10] a) C. A. Denard, H. Huang, M. J. Bartlett, L. Lu, Y. Tan, H. Zhao, J. F. Hartwig, *Angew. Chem. Int. Ed.* **2014**, *53*, 465-469; b) F. Rudroff, M. D. Mihovilovic, H. Gröger, R. Snajdrova, H. Iding, U. T. Bornscheuer, *Nat. Catal.* **2018**, *1*, 12-22.
- [11] a) K. Engstrom, E. V. Johnston, O. Verho, K. P. Gustafson, M. Shakeri, C. W. Tai, J. E. Bäckvall, *Angew. Chem. Int. Ed.* **2013**, *52*, 14006-14010; b) K. P. Gustafson, R. Lihammar, O. Verho, K. Engstrom, J. E. Bäckvall, *J. Org. Chem.* **2014**, *79*, 3747-3751.
- [12] a) E. S. Park, J. S. Shin, *J. Mol. Catal. B-Enzym.* **2015**, *121*, 9-14; b) T. Görbe, K. P. J. Gustafson, O. Verho, G. Kervefors, H. Zheng, X. Zou, E. V. Johnston, J. E. Bäckvall, *ACS Catal.* **2017**, *7*, 1601-1605.
- [13] a) M. Egi, K. Sugiyama, M. Saneto, R. Hanada, K. Kato, S. Akai, *Angew. Chem. Int. Ed.* **2013**, *52*, 3654-3658; b) Y. C. Lee, S. Dutta, K. C. Wu, *ChemSusChem* **2014**, *7*, 3241-3246; c) H. Huang, C. A. Denard, R. Alamillo, A. J. Crisci, Y. Miao, J. A. Dumesic, S. L. Scott, H. Zhao, *ACS Catal.* **2014**, *4*, 2165-2168.
- [14] F. Zhao, H. Li, Y. Jiang, X. Wang, X. Mu, *Green Chem.* **2014**, *16*, 2558-2568.
- [15] Y. Wei, H. Dong, J. Xu, Q. Feng, *ChemPhysChem* **2002**, *3*, 802-808.
- [16] a) D. Feng, T.-F. Liu, J. Su, M. Bosch, Z. Wei, W. Wan, D. Yuan, Y.-P. Chen, X. Wang, K. Wang, X. Lian, Z.-Y. Gu, J. Park, X. Zou, H.-C. Zhou, *Nat. Commun.* **2015**, *6*, 5979; b) Y. Cui, B. Li, H. He, W. Zhou, B. Chen, G. Qian, *Acc. Chem. Res.* **2016**, *49*, 483-493; c) P. Z. Li, X. J. Wang, J. Liu, J. S. Lim, R. Q. Zou, Y. L. Zhao, *J. Am. Chem. Soc.* **2016**, *138*, 2142-2145; d) P. Li, S. Y. Moon, M. A. Guelta, L. Lin, D. A. Gomez-Gualdrón, R. Q. Snurr, S. P. Harvey, J. T. Hupp, O. K. Farha, *ACS Nano* **2016**, *10*, 9174-9182.
- [17] a) Z. Wang, S. M. Cohen, *J. Am. Chem. Soc.* **2007**, *129*, 12368-12369; b) K. K. Tanabe, Z. Wang, S. M. Cohen, *J. Am. Chem. Soc.* **2008**, *130*, 8508-8517; c) A. D. Burrows, C. G. Frost, M. F. Mahon, C. Richardson, *Angew. Chem. Int. Ed.* **2008**, *47*, 8482-8486; d) N. C. Thacker, Z. Lin, T. Zhang, J. C. Gilhula, C. W. Abney, W. Lin, *J. Am. Chem. Soc.* **2016**, *138*, 3501-3509.
- [18] a) L. Chen, H. Chen, R. Luque, Y. Li, *Chem. Sci.* **2014**, *5*, 3708-3714; b) N. Shang, S. Gao, X. Zhou, C. Feng, Z. Wang, C. Wang, *RSC Adv.* **2014**, *4*, 54487-54493; c) A. Aijaz, Q. Zhu, N. Tsumori, T. Akita, Q. Xu, *Chem. Commun.* **2015**, *51*, 2577-2580; d) C. Rösler, R. A. Fischer, *CrytEngComm* **2015**, *17*, 199-217.
- [19] a) Y. Shih, S. Lo, N. Yang, B. Singco, Y. Cheng, C. Wu, I. Chang, H. Huang, C. Lin, *ChemPlusChem* **2012**, *77*, 982-986; b) F. Qin, S. Jia, F. Wang, S. Wu, J. Song, Y. Liu, *Catal. Sci. Technol.* **2013**, *3*, 2761-2768; c) F. Lyu, Y. Zhang, R. N. Zare, J. Ge, Z. Liu, *Nano Lett.* **2014**, *14*, 5761-5765; d) X. Wang, T. A. Makal, H. Zhou, *Aust. J. Chem.* **2014**, *67*, 1629-1631; e) C. Hou, Y. Wang, Q. Ding, L. Jiang, M. Li, W. Zhu, D. Pan, H. Zhu, M. Liu, *Nanoscale* **2015**, *7*, 18770-18779; f) W. Liu, N. Yang, Y. Chen, S. Lirio, C. Wu, C. Lin, H. Huang, *Chem. Eur. J.* **2015**, *21*, 115-119; g) F. Shieh, S. Wang, C. Yen, C. Wu, S. Dutta, L. Chou, J. V. Morabito, P. Hu, M. Hsu, K. C. Wu, C. Tsung, *J. Am. Chem. Soc.* **2015**, *137*, 4276-4279; h) X. Wu, J. Ge, C. Yang, M. Hou, Z. Liu, *Chem. Commun.* **2015**, *51*, 13408-13411; i) J. Mehta, N. Bhardwaj, S. K. Bhardwaj, K. Kim, A. Deep, *Coordin. Chem. Rev.* **2016**, *322*, 30-40; j) P. Li, S. Moon, M. A. Guelta, S. P. Harvey, J. T. Hupp, O. K. Farha, *J. Am. Chem. Soc.* **2016**, *138*, 8052-8055; k) Y. Cao, Z. Wu, T. Wang, Y. Xiao, Q. Huo, Y. Liu, *Dalton Trans.* **2016**, *45*, 6998-7003; l) H. He, H. Han, H. Shi, Y. Tian, F. Sun, Y. Song, Q. Li, G. Zhu, *ACS Appl. Mater. Interfaces* **2016**, *8*, 24517-24524; m) S. Jung, S. Park, *ACS Catal.* **2017**, *7*, 438-442; n) E. Gkaniatsou, C. Sicard, R. Ricoux, J. Mahy, N. Steunou, C. Serre, *Mater. Horiz.* **2017**, *4*, 55-63; o) W. Chen, M.

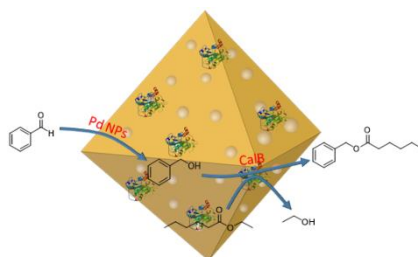
- Vázquez-González, A. Zoabi, R. Abu-Reziq, I. Willner, *Nat. Catal.* **2018**, *1*, 689-695.
- [20] a) M. J. Climent, A. Corma, S. Iborra, M. J. Sabater, *ACS Catal.* **2014**, *4*, 870-891; b) Y. B. Huang, J. Liang, X. S. Wang, R. Cao, *Chem. Soc. Rev.* **2017**, *46*, 126-157; c) R. Limvorapitux, L.-Y. Chou, A. P. Young, C.-K. Tsung, S. T. Nguyen, *ACS Catal.* **2017**, *7*, 6691-6698.
- [21] a) S. Y. Ding, J. Gao, Q. Wang, Y. Zhang, W. Song, C. Su, W. Wang, *J. Am. Chem. Soc.* **2011**, *133*, 19816-19822; b) M. Shakeri, C. Tai, E. Göthelid, S. Oscarsson, J. Bäckvall, *Chem. Eur. J.* **2011**, *17*, 13269-13273; c) C. M. A. Parlett, P. Keshwalla, S. G. Wainwright, D. W. Bruce, N. S. Hondow, K. Wilson, A. F. Lee, *ACS Catal.* **2013**, *3*, 2122-2129; d) L. Li, H. Zhao, J. Wang, R. Wang, *ACS Nano* **2014**, *8*, 5352-5364; e) H. Zhong, C. Liu, Y. Wang, R. Wang, M. Hong, *Chem. Sci.* **2016**, *7*, 2188-2194; f) S. K. Surmiak, C. Doerenkamp, P. Selter, M. Peterlechner, A. H. Schäfer, H. Eckert, A. Studer, *Chem. Eur. J.* **2017**, *23*, 6019-6028; g) Y. Landais, S. Pramanik, V. Liautard, A. Fernandes, F. Robert, M. Pucheault, *Chem. Eur. J.* **2018**, DOI: 10.1002/chem.201803989.
- [22] a) C. Wu, M. Kraume, M. B. Ansorge-Schumacher, *ChemCatChem* **2011**, *3*, 1314-1319; b) K. Gawlitza, C. Wu, R. Georgieva, D. Wang, M. B. Ansorge-Schumacher, R. von Klitzing, *Phys. Chem. Chem. Phys.* **2012**, *14*, 9594-9600.
- [23] Y. Han, S. S. Lee, J. Y. Ying, *Chem. Mater.* **2006**, *18*, 643-649.
- [24] R. Limvorapitux, L. Y. Chou, A. P. Young, C. K. Tsung, S. T. Nguyen, *ACS Catal.* **2017**, *7*, 6691-6698.
- [25] J. Huo, J. Aguilera-Sigalat, S. El-Hankari, D. Bradshaw, *Chem. Sci.* **2015**, *6*, 1938-1943.
- [26] A. Schaate, P. Roy, A. Godt, J. Lippke, F. Waltz, M. Wiebcke, P. Behrens, *Chem. Eur. J.* **2011**, *17*, 6643-6651.
- [27] J. Huo, M. Marcello, A. Garai, D. Bradshaw, *Adv. Mater.* **2013**, *25*, 2717-2722.
- [28] S. J. Garibay, S. M. Cohen, *Chem. Commun.* **2010**, *46*, 7700-7702.
- [29] S. Schmidt, K. Castiglione, R. Kourist, *Chem. Eur. J.* **2018**, *24*, 1755-1768.
- [30] P. Li, J. A. Modica, A. J. Howarth, E. Vargas L, P. Z. Moghadam, R. Q. Snurr, M. Mrksich, J. T. Hupp, O. K. Farha, *Chem* **2016**, *1*, 154-169.
- [31] a) R. M. Blanco, P. Terreros, N. Muñoz, E. Serra, *J. Mol. Catal. B Enzym.* **2007**, *47*, 13-20; b) S. Gao, Y. Wang, T. Wang, G. Luo, Y. Dai, *Bioresour. Technol.* **2009**, *100*, 996-999; c) U. Hanefeld, L. Gardossi, E. Magner, *Chem. Soc. Rev.* **2009**, *38*, 453-468.
- [32] L. Y. Chen, H. R. Chen, R. Luque, Y. W. Li, *Chem. Sci.* **2014**, *5*, 3708-3714.
- [33] A. F. Lee, S. F. J. Hackett, J. S. J. Hargreaves, K. Wilson, *Green Chem.* **2006**, *8*, 549-555.
- [34] S. Wenda, S. Illner, A. Mell, U. Kragl, *Green Chem.* **2011**, *13*, 3007-3047.
- [35] a) H. P. Hemantha, V. V. Sureshbabu, *Org. Biomol. Chem.* **2011**, *9*, 2597-2601; b) S. S. Kotha, N. Sharma and G. Sekar, *Adv. Synth. Catal.* **2016**, *358*, 1694-1698.

Entry for the Table of Contents (Please choose one layout)

Layout 1:

COMMUNICATION

Text for Table of Contents



Yangxin Wang, Ningning Zhang, En Zhang, Yunhu Han, Zhenhui Qi,*
Marion B. Ansorge-Schumacher,* Yan Ge,* Changzhu Wu*

Page No. – Page No.

**Heterogeneous metal-organic
frameworks-based biohybrid
catalysts for cascade reaction in
organic solvent**

Author Manuscript